CRYSTAL GROWTH & DESIGN
2008
VOL. 8, NO. 10
3555–3559

Interconversion of Rutile TiO_2 and Layered Ramsdellite-Like Titanates: New Route to Elongated Mesoporous Rutile Nanoplates

Chih-Wei Peng,[†,‡] Mireille Richard-Plouet,[†] Min-Chiao Tsai,[§] Chi-Young Lee,[§] Hsin-Tien Chiu,*[,‡] Pierre-Emmanuel Petit,[†] Hwo-Shuenn Sheu,[||] Serge Lefrant,[†] and Luc Brohan*[,†]

Institut des Matériaux Jean Rouxel, UMR 6502, 44322 Nantes, France, Department of Applied Chemistry, National Chiao Tung University, Taiwan 30050, R. O. C., Department of Materials Science and Engineering and Center for Nanotechnology, Materials Science and Microsystems, National Tsing Hua University, Taiwan 30043, R. O. C., and National Synchrotron Radiation Research Center, Taiwan 30076, R. O. C.

Received December 1, 2007; Revised Manuscript Received May 8, 2008

ABSTRACT: We report the first soft chemistry synthesis of a new "layered ramsdellite-like" titanate structure, $NaTi_2O_4(OH)$ (lattice parameters: primitive monoclinic system, $a = 4.09$ nm, $b = 0.29$ nm, $c = 0.94$ nm, and $\beta = 80°$), with high-aspect-ratio, platelike morphology (diameter. 20−200 nm; thickness. 10−40 nm; length. 0.05−5 μm) from TiO_2 rutile. The newly prepared titanate can be transformed back to TiO_2 rutile with uniquely shaped mesoporous elongated nanoplate morphology. The reaction proceeds via the disintegration of rutile in NaOH(aq) into $NaTi_2O_4(OH)$. Ion exchange of Na+ in $NaTi_2O_4(OH)$ into H+ forms another new layered ramsdellite-like titanate, $HTi_2O_4(OH)$. A final topotatic condensation of the titanate layers in $HTi_2O_4(OH)$ by heat treatment at relatively low 673 K produces the mesoporous TiO_2 rutile product with highly exposed (110) surfaces.

1. Introduction

Mesoporous titanium dioxide (TiO_2) with good crystallinity has been proposed as the key to improve physicochemical properties of the material.[1] Recently, the synthesis of mesoporous anatase phase TiO_2 has been reported.[2,3] These mesoporous structures, without preferred orientation, were usually synthesized by surfactant-assisted sol−gel processes followed by agglomeration of the as-formed nanoparticles. On the other hand, articles about mesoporous rutile phase TiO_2 were rare and scattered.[4,5] A new methodology has been investigated lately to synthesize TiO_2 with special morphologies.[6] Here, various nanosized titanates can be synthesized by chimie-douce (soft chemistry) routes at low temperatures and converted easily into the nanostructured TiO_2 by appropriate ion-exchange treatments. In this communication, we report the first soft chemistry synthesis of new layered ramsdellite-like titanate structures with high aspect ratio platelike morphology from TiO_2 rutile. More importantly, the newly prepared titanates can be transformed, via a simple chimie-douce method at low temperature, back to rutile TiO_2 with uniquely shaped mesoporous one-dimensional (1D) nanoplate morphology.

2. Experimental Section

Preparation of $NaTi_2O_4(OH)$, A. To NaOH(aq) (10 M, 10 mL), TiO_2-rutile (1.0 g, 13 mmole, Riedel-de-Haën, diameter <3 μm) was added. The mixture was transferred to a 50 mL Teflon-lined autoclave and heated to 493 K for 72 h. The material was washed with distilled water and then filtered. The steps were repeated until pH was below 12. After centrifuged and dried at 343 K in air, **A** (1.3 g, 6.5 mmol, 50% yield based on TiO_2) was isolated.

Preparation of $HTi_2O_4(OH)$, B. A (1.0 g, 5.0 mmol) was stirred in HCl(aq) (0.1 M, 50 mL) for 2 h. The material was then filtered, washed with distilled water repeatedly until the pH was above 6, and collected by centrifuging. After being dried at 343 K in air, **B** (0.80 g, 4.5 mmol, 90% yield based on **A**) was obtained.

Preparation of Mesoporous TiO_2-rutile, C. B (0.50 g, 2.8 mmol) was heated at 673 K (ramp rate, 10 K min^{-1}) for 4 h in air to form **C** (0.45 g, 2.8 mmol, 100% yield based on **B**).

Characterization. Scanning electron microscopic (SEM) images were obtained by using a JEOL 6400F with a tungsten cathode field emission gun operated at 10 keV. X-ray diffraction (XRD) data were collected on a Siemens D5000 diffractometer with Cu Kα radiation in Bragg−Brentano geometry and on the National Synchrotron Radiation Research Center (NSRRC, Taiwan) beamline C01 (power: 13 keV, wavelength: 0.09537 nm) as the incident X-ray source. Transmission electron microscopic (TEM) studies were performed on a Hitachi HF2000 with a field-emission electron source at 200 keV. For TEM studies, samples prepared by grinding solid products followed by dispersing them in ethanol were placed on holey or lacey carbon films on copper grids. Energy-dispersive X-ray (EDX) studies were performed by using a Kevex X-ray analysis probe attached to a JEOL 5800LV SEM with a conventional tungsten electron source operating at 15 keV. The EDX samples were prepared by pressing 100 mg of powder into a pellet with 8 mm diameter and 1−2 mm thickness. Thermogravimetric analyses coupled to mass spectrometry (TGA-MS) studies were carried out using a SETARAM TG-DSC 111 equipment fitted with a mass spectrometer Leybold Inficon. The analysis was operated at 273−1073 K with a heating rate of 5 K min^{-1} in Ar environment. The specific surface area determined from the Brunauer−Emmett−Teller equation (BET method) was performed by N_2 adsorption at 77 K (under liquid nitrogen) using a Micromeritics ASAP 2010.

X-ray Absorption Spectroscopic (XAS) Studies. XAS spectra were collected at the titanium K-edge in transmission mode on the European Synchrotron Radiation Facility (ESRF, Grenoble) bending magnet beamline BM29, in the range 4750−5820 eV. For extended X-ray absorption fine structure (EXAFS) spectra, the $k\chi(k)$ function was extracted from the absorption coefficient using XAFS program with a cubic spline function.[7] The Fourier transforms (FT) were performed using kχ(k) with a Kaiser−Bessel window ($\tau = 3$) in the k-range 3.6−12.5 $Å^{-1}$. Using the FEFF7 code,[8] we calculated EXAFS oscillations for different clusters corresponding to usual Ti−O and Ti−Ti distances, namely in the 1.90−2.20 Å range for the first shell and between 3.15 and 3.80 Å for the second shell, corresponding to connection between octahedra sharing edges or corners. All the fits

* Corresponding author. E-mail: htchiu@faculty.nctu.edu.tw (H.-T.C.); luc.brohan@cnrs-imn.fr (L.B.).
[†] Institut des Matériaux Jean Rouxel.
[‡] National Chiao Tung University.
[§] National Tsing Hua University.
[||] National Synchrotron Radiation Research Center.

10.1021/cg701183a CCC: $40.75
Published on Web 08/29/2008

Table 1. Summary of the Samples

sample	empirical formula	preparation	morphology	dimensions (nm) width	thickness	length	phase	specific surface (m^2 g^{-1})
A	$Na(Ti_2O_4)OH$	RDH TiO_2 rutile (diameter <3 μm) in 10 M NaOH(aq), 493 K, 72 h in autoclave	1D nanoplates	20−200	10−40	50−5000	layered ramsdellite[a]	70
B	$H(Ti_2O_4)OH$	**A** in 0.1 M HCl(aq), 298 K, 2 h	1D nanoplates	20−200	10−40	50−5000	layered ramsdellite	75
C	TiO_2	**B** at 673 K, 4 h	mesoporous 1D nanoplates	10−200	5−20	50−5000	rutile	43[b]

[a] Proposed name to describe the new layered titanate structure. [b] With BJH adsorption cumulative surface area of pores, 34 m^2 g^{-1}; and average pore diameter, 11.3 nm.

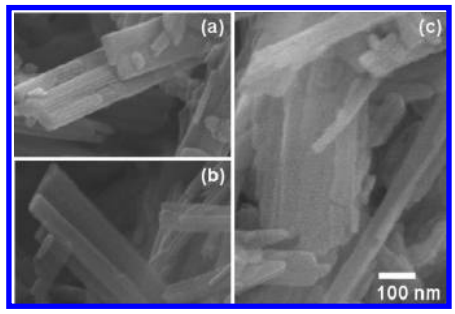

Figure 1. SEM images of (a) **A**, sodium titanate obtained from TiO_2 rutile at 493 K; (b) **B**, proton-exchanged titanate; and (c) **C**, mesoporous rutile.

were undertaken with Michalowicz's EXAFS signal treatment and refinement programs while the reduction factor S_0^2 was fixed to 1.[9]

3. Results and Discussion

Commercial rutile TiO_2 powders dispersed in 10 M $NaOH_{(aq)}$ solution was heated in an autoclave at 493 K for 72 h. The isolated solid was rinsed with deionized water and dried at 343 K to give a white powder **A**. **A** was immersed in 0.1 M HNO_3(aq), rinsed with deionized water, and dried at 343 K under air to produce an H+ exchanged product **B**. Heating **B** at 623 K in air for 4 h produced a solid phase **C** as the final product. Detailed experimental conditions for samples preparation and morphological properties are summarized in Table 1.

SEM images in Figure 1 show the morphology of **A**, **B**, and **C**. As shown in Figure 1a, **A** is composed of one-dimensional (1D) platelike products, with width 20−200 nm, thickness 10−40 nm, and length 0.05−5 μm. After the H^+-exchange and the post-heat-treatment steps, products **B** and **C** retain the overall morphology and dimensions of **A**, as indicated in images b and c in Figure 1.

BET experiments showed that specific areas of **A**, **B**, and **C** were 70, 75 and 43 m^2g^{-1}, respectively. Barrett−Joyner−Halenda (BJH) estimation also indicated that **C** was mesoporous with an average pore diameter of 11.3 nm and a pore area of 34 m^2g^{-1}. We employed EDX spectroscopy and TGA/MS to study the chemical composition of the as-prepared samples. From the EDX results, we discovered that **A** contained Na and Ti atoms with the Na/Ti ratio close to 0.5, whereas **B** and **C** were Na-free. By assuming that all Ti atoms would transform into TiO_2 after the heat treatment, we estimated that the H_2O/TiO_2 ratios were 0.25 and 0.50 for **A** and **B**, respectively, using the TGA/MS data. Thus, we are able to express the empirical formula of **A** and **B** to be "$NaHTi_2O_5$" and "$H_2Ti_2O_5$", respectively. We also discovered that **C** was essentially dehydrated.

The XRD patterns in Figure 2 reveal that **A** and **B** have closely related crystal structures. The differences are that the peaks of **B** are broader and lower in intensities than those of **A**.

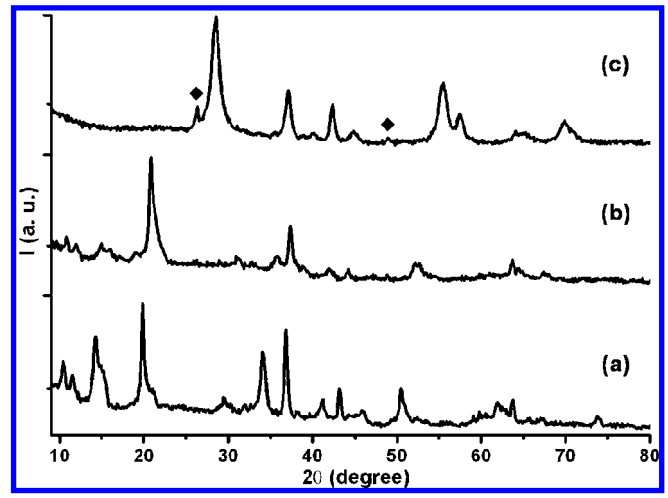

Figure 2. Powder XRD of (a) **A**, (b) **B**, and (c) **C**. (◆, the reflection peaks of anatase).

This indicates that **B** is less ordered. In addition, the peaks of **B** have higher 2θ values than the corresponding ones of **A** do. This suggests that at least one axis in the unit cell of **B** is shorter than the equivalent one of **A**. The XRD patterns of both samples could not be assigned to any known titanate structures. In addition, peaks below 5° are observed for both. This implies that each of them possesses a long axis in the unit cell. The XRD pattern of **C** indicates that it contains rutile (JCPDS #89−4920) and anatase (JCPDS #89−4921) TiO_2 as the major and minor components. In addition, the peaks exhibit large width of half-height. This suggests that **C** is composed of small grain size crystallites. It is intriguing to note that through the dehydration of **B** at 623 K, the material could be transformed back to TiO_2 rutile phase. Below, we will discuss in the TEM studies how to index the reflection peaks and to determine the lattice parameters.

TEM Studies of Ramsdellite-Like Titanates. The TEM images shown in Figure 3 reveal that **A**, **B** and **C** are composed of dispersed 1D high-aspect-ratio thin nanoplates. The overall morphology agrees with the SEM data shown in Figure 1. As discussed in the XRD observations above, one crystallographic parameter of **A** close to 4 nm in its unit cell. We assume this long axis to be a^*. From the selected area electron diffraction (SAED) pattern and the fringes shown in the high-resolution TEM (HRTEM) image of **A** in Figures 3(a) and 3(b), the distance of (010) and (001) is identified to be 0.29 and 0.94 nm. These are typical features of TiO_2 ramsdellite (TiO_2(R)) (JCPDS #82−1123).[10,11] This arrangement was encountered for MnO_2 and TiO_2 and has been reported to be a good electrode material in lithium ion battery.[12] The TEM observation implies that the new type sodium titanate **A** probably has a structure with (b, c)* planes similar to those of ramsdellite. For further structural information, the reciprocal lattice of a sample was

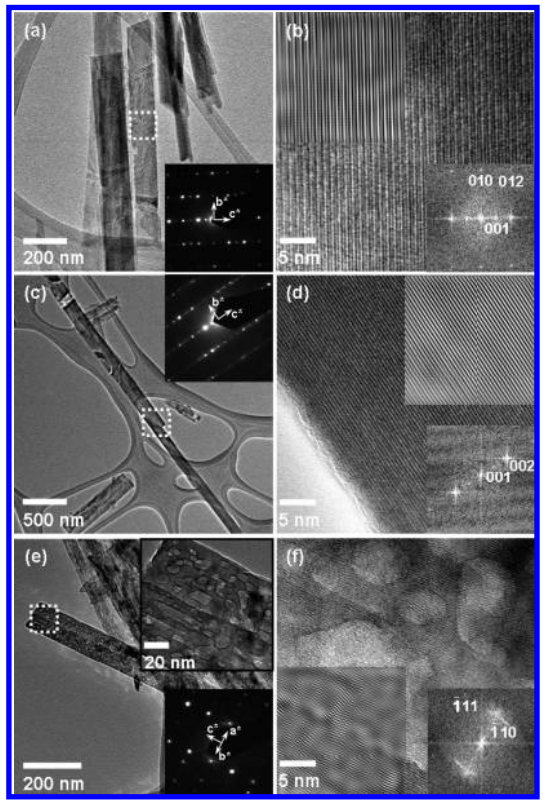

Figure 3. (a) TEM and SAED (inset, from the dotted square) and (b) HRTEM, FT, and reversed-FT results (insets) of **A**, $NaTi_2O_4(OH)$, viewing along [100]; (c) TEM and SAED (inset, from the dotted square), and (d) HRTEM, FT, and reversed-FT results (insets) of **B**, $HTi_2O_4(OH)$, viewing along [100]; (e) TEM and SAED (inset, from the dotted square), and (f) HRTEM, FT, and reversed-FT results (insets) of **C**, TiO_2 rutile, viewing along [110].

reconstructed by using a Philips CM30 TEM with a double-tilt sample holder. By tilting along the b^* axis (range = ±60°) of a well-isolated crystallite, several oriented SAED patterns could be sequentially recorded. We reconstructed the 2D reciprocal lattice in the (a^*, c^*) plane and found the lattice parameters of **A**: $a = 4.09$ nm, $b = 0.29$ nm, $c = 0.94$ nm, and $\beta = 80°$. On the basis of the data, the structure of **A** is determined to crystallize in a primitive monoclinic system. The large value of a implies that **A** has a "layered ramsdellite-like" structure. Taking into account the EDX and TGA/MS results, the formula of **A** is inferred to be $NaTi_2O_4(OH)$. In Figure 3c, the HRTEM image and SAED of **B** exhibit patterns and distances of (010) and (001) planes close to those of **A**. This implies that the b and c parameters, 0.29 and 0.94 nm, respectively, are essentially unchanged after the proton-exchange process. From the XRD result obtained on a synchrotron radiation beam line, the lattice parameter a of **B** was calculated to be 3.63 nm, which is shorter than that of **A** and responsible for the "right-shift" of the XRD peaks. It is understandable since the Na+ ions intercalated in the titanate layers were replaced by the H+ ions. Based on the information discussed above, the formula of **B** is proposed to be $HTi_2O_4(OH)$. However, satisfactory Rietveld refinement results were difficult to achieve due to many available (*hkl*) indexations for an apparent peak. The origins may be from broad peak widths, large cell parameters and insufficient structural information. We could not improve the analysis appreciably even the X-ray from a synchrotron radiation beam line was used as the source. More detailed lattice parameters of **A** and **B** would be obtained when better quality X-ray diffraction results are available.

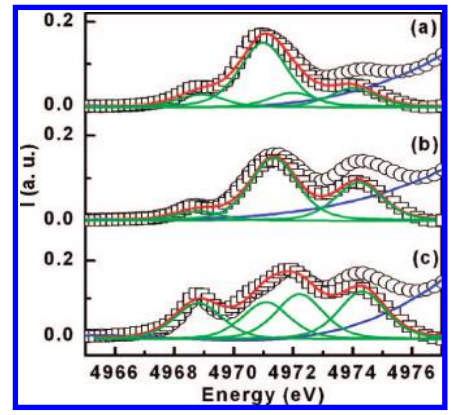

Figure 4. XAS pre-edge peaks for (a) sample **A**, (b) rutile, and (c) anatase. (○, original data; □, baseline adjusted data; blue line, baseline; green line, components fitted with Gaussian function; red line, sum of the green components).

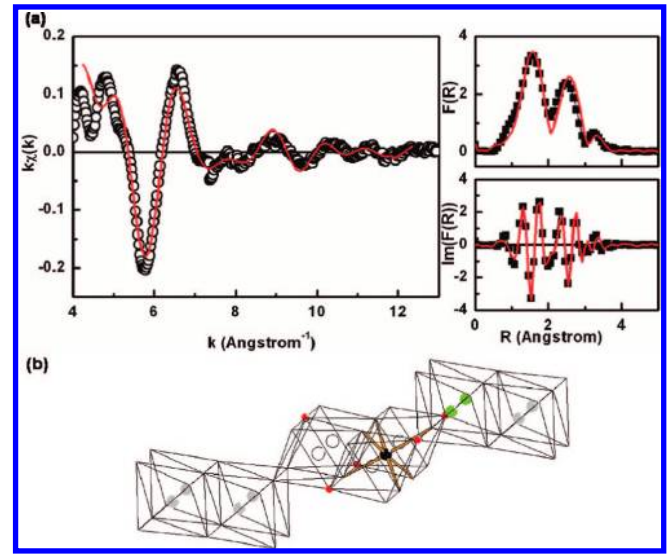

Figure 5. (a) Experimental (filtered) and calculated (red line) EXAFS spectra of **A**. (Left) Inverse FT, module of the FT (upper right), and imaginary part (lower right). (b) Schematic view of Ti neighboring atoms for ramsdellite type-structures along the a-axis. Black dot, the Ti absorber; white, red, and green dots refer to the second Ti, the third O, and the fourth Ti shells, respectively.

Table 2. Results of EXAFS Refinements for A[a]

shell	element	N	$\sigma \times 10^2$	R (Å)	ΔE (eV)
1	O	6(1)	10.5	1.96 (5)	−2.5
2	Ti	3.7(7)	9.8	3.01 (5)	−2.5
3	O	6.3(1.2)	9.8	3.52 (5)	−2.5

[a] $\rho = 2.1 \times 10^{-2}$; $\chi_v^2 = 7.6 \times 10^{-3}$.

EXAFS Studies of Ramsdellite-Like Titanates. Information concerning the local symmetry around Ti atoms can be inferred from the XANES spectra and particularly from the pre-edge structure analyses (Figure 4). The refined positions of XANES of **A** were compared to those of anatase and rutile. Their three peaks can be decomposed into four components noted A1, A2, A2′, and A3, near 4969, 4971, 4972, and 4974 eV, respectively. This implies that the local symmetry around Ti atoms in **A** is similar to anatase (D_{2d} group). However, the intensity of peak A2 with respect to peak A2′ in **A** is larger than those observed in anatase. This suggests that **A** may contain small anatase-like crystalline domains.[13] It was reported that 5-fold coordinated Ti atoms showed a pre-edge peak at 4970.5 eV.[14] Its height

Scheme 1. Proposed Chimie-Douce Pathway to Convert Bulk Rutile TiO_2 to (110)-Exposed Rutile TiO_2[a]

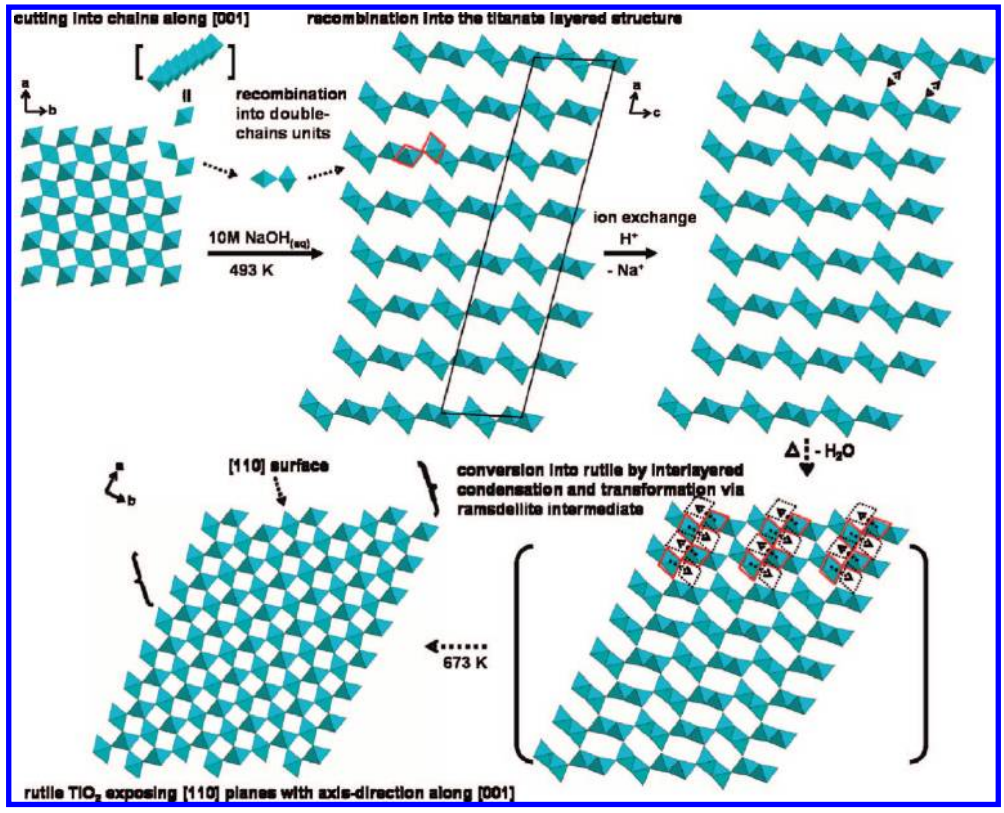

[a] The red-framed parts show the transformation of migrating units after the condensation.

reached half the height of the signal in the first EXAFS oscillation. In contrast, the height of the corresponding signal of **A** (the A1 peak) is only one-third of the first EXAFS oscillation. This is characteristic of Ti atoms in an octahedral oxygenated environment. Therefore, during further EXAFS signal analysis in Figure 5a, which provides information about the coordination number and the distances of different shells around the Ti atoms, the number of oxygen atoms as the first neighbors can be fixed to six. On the basis of the XRD and TEM observations mentioned above, we propose a "layered" ramsdellite structural model for **A**. The local environment of Ti atoms in **A** is plotted in Figure 5b. The structure exhibits a layered arrangement derived from the tunnels of ramsdellite structure. The sheets are composed of infinite ribbons, which is the result of double chains of edge-sharing octahedra. Each ribbon is linked to the other by sharing corners through μ_3 oxygen atoms in the perpendicular direction to form a layer. In Figure 5a, the inverse Fourier transforms of the experimental result (the squared dot line) and the calculated spectra (the red line) are compared. The refinement results are shown in Table 2. This result is coherent with the proposed model.

TEM Studies of Mesoporous Rutile TiO_2. The TEM images of **C** are shown in Figures 3(e) and 3(f). They suggest that while retaining the high-aspect-ratio platelike morphology of **A** and **B**, **C** contains many mesopores with diameters 2 − 20 nm. This observation agrees well with the BJH result. The mesopores were probably generated during the dehydration-condensation of **B** during heat treatment. The process could remove water molecules from **B** and create empty spaces by shrinking the adjacent materials. An HRTEM of **C** in Figure 3f shows that the fringes with a distance of 0.33 nm are slightly disordered. By analyzing the SAED in the inset of Figure 3e and Fourier-transforming a selected area in the HRTEM in Figure 2f, we discover that the simulated diffraction pattern in Figure 2f agrees with that of rutile TiO_2 (JCPDS #89−4920) viewing along the ^{110}* direction. This agrees well with the XRD result. Besides, the axis-direction of the sample is along [001]*. The fringes in Figure 2f can be assigned to the (110) planes. The bracketlike (110) diffraction ring pattern confirms the presence of the slightly disordered structure. Similar to the mesopore formation, we propose that the slightly disordered structure was also produced during the dehydration-condensation process. In addition, we investigated many different areas on the sample in Figure 3e. We found that all viewings were along [110]*. The observation suggests that the nanocrystallite preferentially grow along [110]. On the basis of these observations, we propose that the rutile (110) surfaces are highly exposed in **C**. In photoinduced processes on rutile TiO_2 surface, (110) planes are regarded as the ones providing more active sites.[15]

Proposed Conversion Pathway. To interpret how the (110)-exposed mesoporous rutile TiO_2 formed, an illustration is proposed in Scheme 1. It suggests a pathway to show how bulk rutile is converted into (110)-exposed rutile TiO_2 nanoplates via a fragmentation-recombination route. In the first step, the initial commercial rutile is degraded by concentrated NaOH(aq) into titanate double-chain building blocks. This double chain is formed of two ribbons of octahedral sharing edges; the ribbons are connected by corners through μ_3 oxygen atoms. This is common to rutile and ramsdellite. These building blocks then recombine by sharing edges into the new type layered ramsdellite-like titanate, $NaTi_2O_4(OH)$, although the true symmetry of the material is yet to be fully solved. After the Na+ ions are replaced by H+ ions, the other new type layered ramsdellite-like titanate, $HTi_2O_4(OH)$, is obtained. Finally, we propose a topotatic condensation process which removes H_2O molecules and reconnects the titanate layers into a ramsdellite TiO_2

intermediate. Because ramsdellite is known for its easy transformation into rutile phase at temperatures below 473 K,[16] we assume the as-formed intermediate is converted directly to the final rutile product. This process would generate rutile with a preferred orientation in ^{110} direction as the titanate layers of $HTi_2O_4(OH)$ are reconnected by condensation. The multistep condensation process could shrink the titanate layer distance also. This rationalizes how the mesopores and the turbostratic (110) planes are generated in the 1D rutile TiO_2 nanoplates.

4. Conclusion

In conclusion, a new chimie-douce route based on the acido-basic approach to transform bulk rutile TiO_2 into 1D mesoporous rutile nanoplates is discovered. The reactions proceed via the disintegration of rutile in NaOH(aq) into a new type "layered ramsdellite-like" sodium hydroxo titanate, $NaTi_2O_4(OH)$, and the ion exchange of Na+ in $NaTi_2O_4(OH)$ into H^+ to form another new "layered ramsdellite-like" titanate, $HTi_2O_4(OH)$. A final condensation of the titanate layers of $HTi_2O_4(OH)$ by heat treatment at relatively low 673 K produces the unique 1D mesoporous rutile product with highly exposed (110) surfaces. These newly synthesized materials may exhibit unique properties in photocatalysis and electrochemical devices. Related investigations are in progress.

Acknowledgment. We thank NSC, MOE, and NSRRC (Hsinchu) of Taiwan, the Republic of China, and CNRS of France for support. We also acknowledge ESRF (Grenoble) for provision of beamtime (Project CH-2220) and we thank Dr. Carmello Prestipino (BM29) for assistance in using the beamline.

Supporting Information Available: TGA/MS and XRD of $NaTi_2O_4(OH)$ and $HTi_2O_4(OH)$; HRTEM image and reciprocal lattice of $NaTi_2O_4(OH)$; XAS study (PDF). This material is available free of charge via the Internet at http://pubs.acs.org.

References

(1) Carp, O.; Huisman, C. L.; Reller, A. *Prog. Solid State Chem.* **2004**, *32*, 33.
(2) Moser, J.; Gratzel, M. *J. Am. Chem. Soc.* **1983**, *105*, 6574.
(3) Yanagisawa, K.; Ovenstone, J. *J. Phys. Chem. B* **1999**, *103*, 7781.
(4) Samuela, V.; Muthukumara, P.; Gaikwadb, S. P.; Dhageb, S. R.; Ravib, V. *Mater. Lett.* **2004**, *58*, 2514.
(5) Yu, N.; Gong, L.; Song, H.; Liu, Y.; Yin, D. *J. Solid State Chem.* **2007**, *180*, 799.
(6) Peng, C.-W. Joint Ph. D. Thesis, National Chiao Tung University and Université de Nantes, Hsinchu, Taiwan, and Nantes, France, 2006.
(7) WintererM. XAFS A Data Analysis Program for Material Sciences. In *Proceedings of the 9th International Conference on X-ray Absorption Fine Structure (XAFS-IX)*; Grenoble, France, Aug 26−30, 1997; Goulon, J., Goulon-Ginet, C., Brookes, N. B. , Eds.; Published in *J. Physique IV* **1997**, *7*, C2-243.
(8) Rehr, J. J.; Mustre de Leon, J.; Zabinsky, S. I.; Albers, R. C. *J. Am. Chem. Soc.* **1991**, *113*, 5135.
(9) Michalowicz, A. *Logiciels Chim., Soc. Fr. Chim.* **1991**, 102.
(10) Marchand, R.; Brohan, L.; Tournoux, M. *Mater. Res. Bull.* **1980**, *15*, 1129.
(11) Akimoto, J.; Gotoh, Y.; Oosawa, Y.; Nonose, N.; Kumagai, T.; Aoki, K.; Takei, H. *J. Solid State Chem.* **1994**, *113*, 27.
(12) Gover, R.; Tolchard, J.; Tukamoto, H.; Murai, T.; Irvine, J. *J. Electrochem. Soc.* **1999**, *146*, 4348.
(13) Hanley, T. L.; Luca, V.; Pickering, I.; Howe, R. F. *J. Phys. Chem. B* **2002**, *106*, 1153.
(14) Farges, F.; Gordon, E.; Brown, Jr.; Rehr, J. *J. Phys. Rev. B* **1997**, *56*, 1809.
(15) Bredow, T.; Jug, K. *Surf. Sci.* **1995**, *327*, 398.
(16) Takahashi, Y.; Kijima, N.; Akimoto, J. *Chem. Mater.* **2006**, *18*, 748.

CG701183A